

Accurate Calibration of VLBI Measurements of Circular Polarization

W. D. Cotton December 10, 2010

Abstract—A technique is described for making high accuracy Stokes V calibration of VLBI observations of strong maser sources. This is an adaptation of traditional self calibration techniques and is based on the assumption that the net Stokes V in the maser spots is zero when averaged over the whole spectrum. The dynamic range of images derived using this technique can also show dramatic improvements. The technique is applied to VLBA observations of SiO masers in the AGB star IK Tau. Solid detections of Stokes V are obtained although it is unclear if the circular polarizations arises from Zeeman splitting or another effect.

Index Terms—Interferometric calibration, SiO maser

I. INTRODUCTION

MEASUREMENTS of circular polarization using antennas with feeds sensitive to Right- and Left-hand circular polarization require particularly accurate calibration as the effect sought is the small difference of large and independently measured values. The problem is particularly acute when the antennas used are similar to those in the VLBA or EVLA in which the feeds are located off axis; the “beam squint” resulting from this arrangement gives rise to an instrumental circular polarization that varies with location in the beam, hence with pointing error. This memo discusses the modification of traditional self-calibration techniques to the case of interferometric measurements of maser sources and applies the technique to observations of the SiO masers in an evolved star. The technique discussed is implemented in the Obit package ([1], <http://www.cv.nrao.edu/~bcotton/Obit.html>).

II. CALIBRATION OF CIRCULAR POLARIZATION OF MASERS

Circular polarization (AKA Stokes parameter V) can be measured by an interferometer detecting the Right- and Left-handed circularly polarized signals by subtracting the Right-Right (RR) correlations from Left-Left (LL). The circularly polarized component of celestial signals is usually very small compared the the total intensity requiring very accurate relative calibration of the RR and LL correlations to recover meaningful measurements of the circular polarization. In practice, the RR and LL systems are calibrated independently. In the case of VLBI, there are no usable calibration sources and the amplitude calibration is usually based on measurements of the system temperature and the antenna gains resulting in relative gain errors on the order of a percent or more.

For strong maser sources, especially at high frequencies where antenna pointing is more difficult, the technique of “template fitting” is beneficial. This technique uses a reference single dish spectrum in each RR and LL and uses the autocorrelation spectra at each antenna to determine time dependent gains for each antenna and correlation product by determining the gain that results in the best match of the observed spectra to the reference spectra. This is very useful for removing opacity and pointing variations but is still limited by the accuracy of the cross calibration of the reference spectra. As these are generally calibrated independently, there will be a residual systematic difference.

Amplitude self calibration has traditionally been used to cross calibrate RR and LL amplitude systems. This technique is to determine the gains needed to align the observations to a given sky model. This requires that the sky model, including any circularly polarized component be known. For continuum observations Stokes V can be assumed zero to a good approximation. However, if the determination of the Stokes V component is desired, such an assumption is inadequate.

The traditional approach to calibrating the phases of VLBI maser observations is to self calibrate a single channel and apply the derived gains to all channels. This works well for phase calibration but if applied to amplitudes, will remove the signature of any circular polarization in that channel; possibly inserting it into others.

Effects like weak Zeeman splitting which introduce minor frequency shifts between RR and LL components of lines should produce circular polarization with a net of zero when averaged over the whole spectrum. However, the brightness distribution of a maser source changes dramatically across the spectrum and cannot be described by a single sky model as is the practice in traditional self calibration.

III. SELF CALIBRATION USING A FREQUENCY DEPENDENT SKY MODEL

As just described, traditional self calibration uses a single sky model to calibrate a data set. However, a frequency dependent sky model (the CLEAN components of the final spectral image cube) can be used to calibrate such a data set. The self calibration technique used in the Obit package as well as AIPS is to divide the observations by the Fourier transform of the sky model, average all channels and determine the gains needed to convert the model divided data to (1.0,0.0). It is a relatively straightforward adaptation to divide each channel by an independent sky model before averaging channels. This is the technique implemented in the Obit task MzrCal.

A frequency dependent sky model has other benefits in addition to cross calibration of amplitude, the sensitivity of the

whole spectrum is used in determining the gain calibration. This results in better calibration, hence dynamic range than calibration determined from a single channel.

IV. APPLICATION OF TECHNIQUE: IK TAU

The multichannel self calibration technique was applied to VLBA observation of two SiO maser transitions near 43 GHz in the evolved star IK Tau. The data were recorded in two 8 MHz frequency windows centered on the 42.8 and 43.1 masing transitions of SiO in right and left hand circular polarization. Correlation used the new NRAO VLBA DifX correlator in the AOC in Socorro, NM and produced all cross and auto correlation products using 1024 channels of 7.8 kHz bandwidth (~ 54 m/s velocity resolution). Initial processing and calibration followed the method described in [2] and included standard calibration based on system temperatures, antenna gain curves, weather information and template fitting. Continuum calibrators were used to calibrate group delay and linear polarization.

Final self-calibration and imaging used Obit tasks Calib, MazrCal and Imager and consisted of the following steps in each transition:

1) **Single channel self calibration**

The initial phase calibration was based on a single channel image (actually average of five adjacent channels) derived by traditional self-calibration using a solution interval of 4 seconds. This calibration was applied and the 350 channels centered on the maser emission were imaged with a running average of 3 channels to improve sensitivity.

2) **First multi channel phase self calibration**

The inner 300 channels of the image cube derived in the previous step were used in MazrCal to derive a refined phase calibration. This calibration was used to make an improved image cube as before.

3) **Second multi channel phase self calibration**

The inner 300 channels of the image cube derived in the previous step were used in MazrCal to derive a further refined phase calibration. This calibration was used to make an improved image cube as before.

4) **Apply phase calibration**

The calibration from the previous step was applied to the data and a new dataset created.

5) **Multi channel amplitude and phase self calibration**

The inner 300 channels of the image cube derived in the previous imaging step were used in MazrCal to derive an amplitude and phase gain calibration using a solution interval of 2 minutes.

6) **Final imaging**

Final imaging was done in two passes, the first imaging Stokes I forcing the use of both RR and LL correlations (Stokes "F" in Imager) and Stokes V. Imaging used the full spectral resolution of the data. This forces identical uv coverage and beams for Stokes I and V allowing a better comparison. The second imaging was of Stokes I, Q and U.

The improvement in image quality during this process is illustrated in Figure 1 and Table I. These describe the

TABLE I
EFFECT OF SELF-CALIBRATION ON DYNAMIC RANGE

Stage	Dynamic range
Single channel phase	73
First multichannel Phase	113
Second multichannel Phase	122
Multichannel Amp & Phase	313

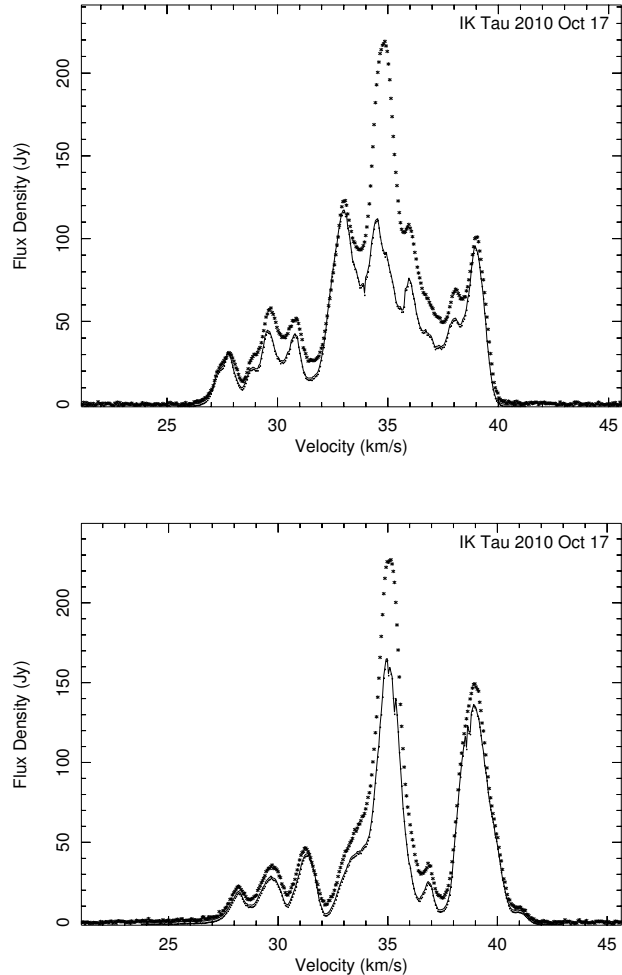


Fig. 2. Spectra of IK Tau, stars (*) show the reference single dish spectrum, the solid line is derived from the interferometric images. The top is the $\nu=2$, $J=1-0$ transition of SiO at 42.8 GHz and the bottom is the $\nu=1$, $J=1-0$ transition of SiO at 43.1 GHz.

improvement in the dynamic range in a single plane at various stages in the processing. This processing took roughly a day for each transition on a fast work station.

V. IK TAU RESULTS

The summed image and single dish spectra are shown in Figure 2. Elliptical rings were fitted to the combined Stokes I images as described in [2] and are given in Table II along with previous measurements from [2]. Combined Stokes I images, combined linear polarization and velocity fields are given in Figure 3 also illustrating the fitted ellipses.

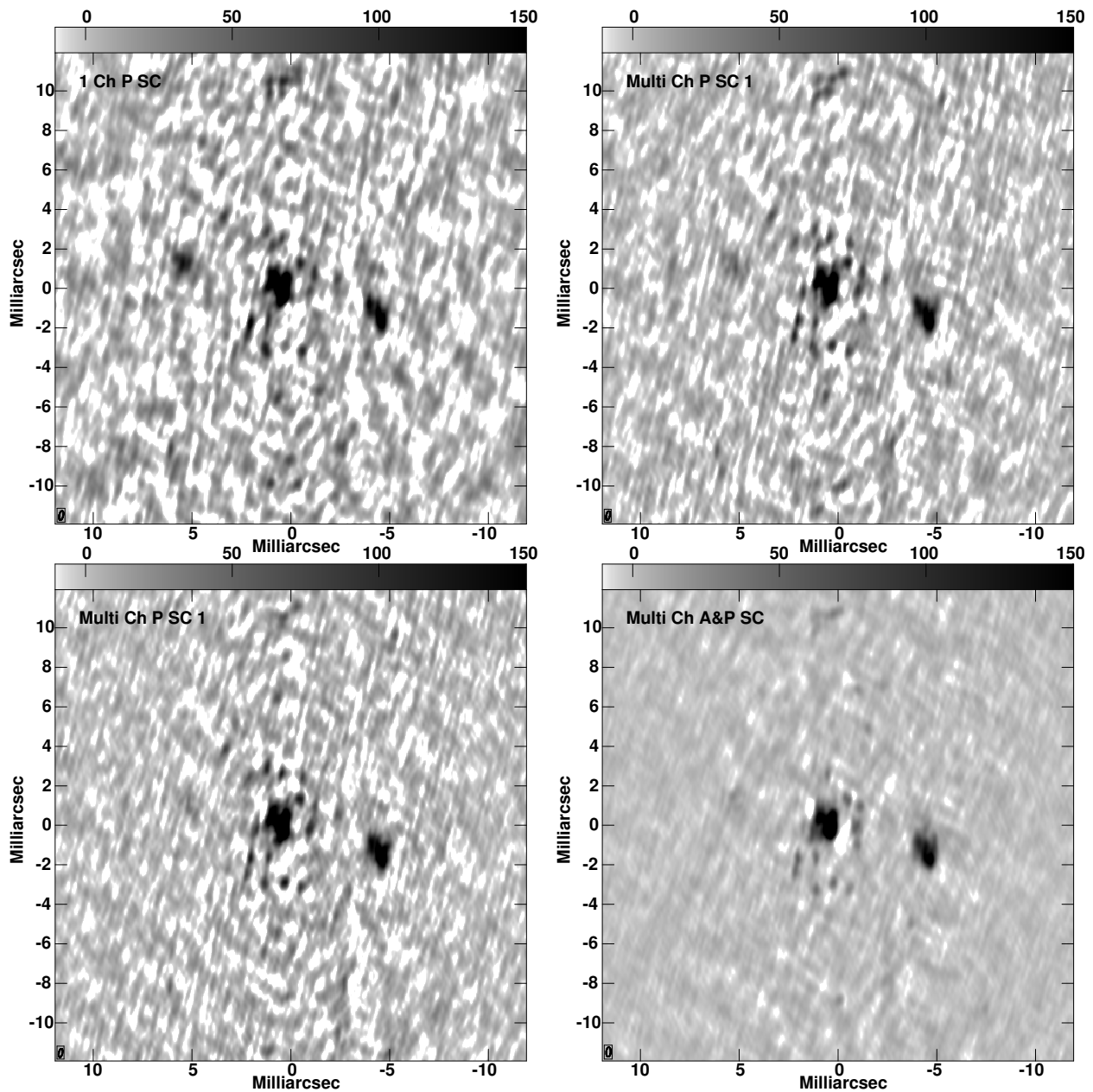


Fig. 1. Close up of a region of one spectral channel at various stages of self calibration. Displayed are the same range of flux densities relative to the image peak; Scales on top give values in units of 0.001. Top left only used phase self cal with a single channel image. Top right is with one iteration of multi channel phase self cal; Bottom left is with a second phase only multi channel self calibration and Bottom right is the final image with a multi channel amplitude and phase self calibration.

The polarization results for the $\nu=2$, $J=1-0$ transition at 42.8 GHz are shown in Figure 4. Pixel spectra in Stokes I, linear and circular polarizations at selected locations are given in Figures 5 and 6. Similar results for the $\nu=1$, $J=1-0$ transition at 43.1 GHz are given in Figures 7, 8 and 9.

VI. DISCUSSION

Use of the technique of a sky model per spectral channel appears to be an effective technique for improving the dynamic range of VLBA maser images. In the example case shown, the dynamic range was improved from 73 to over 300. The roughly equal amounts of positive and negative values in the Stokes V images show that any residual instrumental

circular polarization has been reduced to well below the level of actual circular polarization from the source. While the circular polarization spectra of some maser spots show the expected symmetric “S” shape from Zeeman splitting, not all do; many appear hard to reconcile with Zeeman splitting, even in complex regions. The technique may not work well for masers such as those from the OH molecule for which the Zeeman splitting is very strong resulting in very different RR and LL spectra.

REFERENCES

- [1] W. D. Cotton, “Obit: A Development Environment for Astronomical Algorithms,” *PASP*, vol. 120, pp. 439–448, 2008.

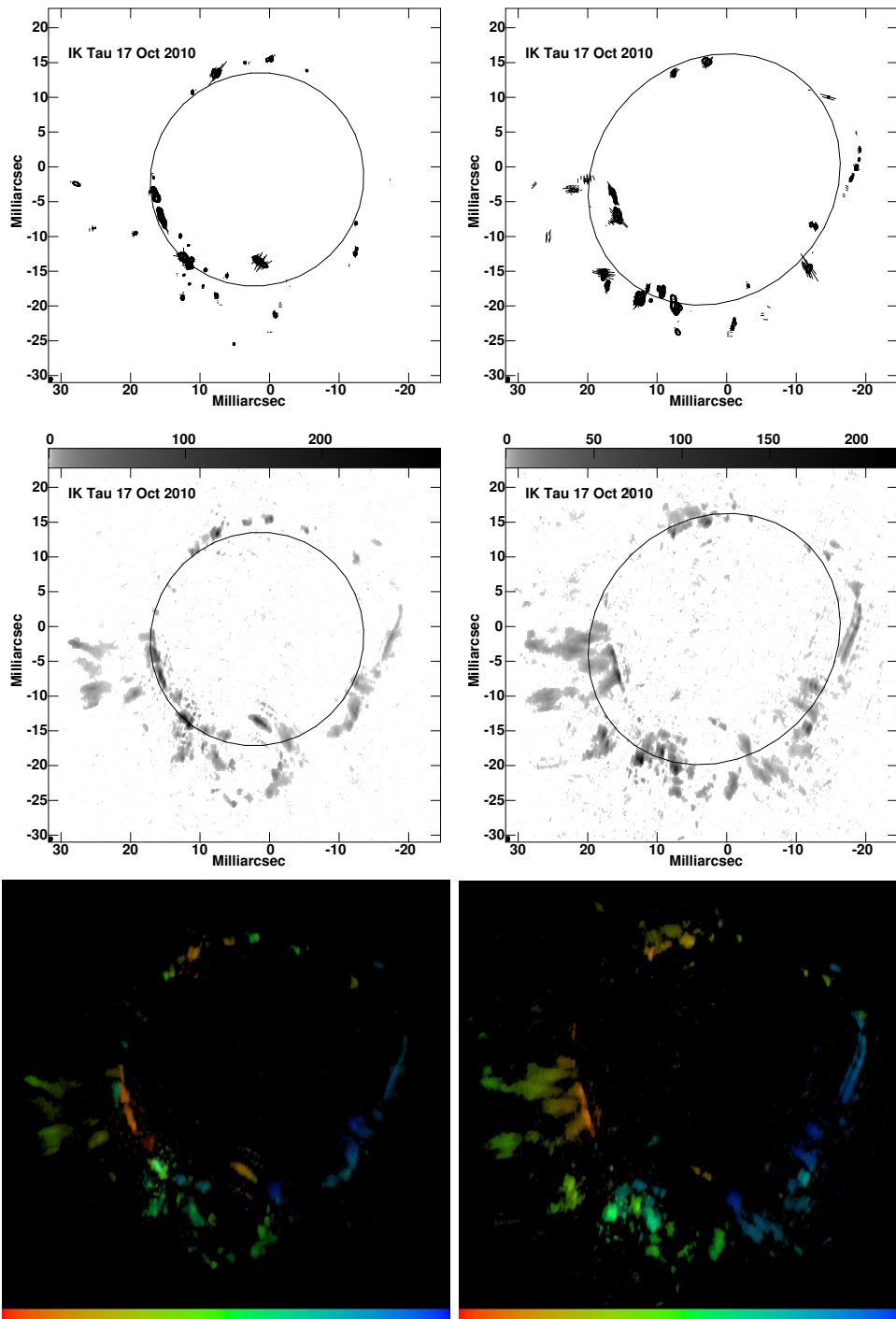


Fig. 3. Images of IK Tau, 17 Oct 2010. The left column is the $\nu=2$, $J=1-0$ transition at 42.8 GHz and the right column is $\nu=1$, $J=1-0$ at 43.1 GHz. The top figures show total intensity contours at powers of 2 times the RMS with polarization E-vectors superposed. The ellipses represent the fits to the maser ring. The middle figures are the square root of the total intensity as a gray scale with the scale in Jy/beam given at the top; the circles give the location and size of the fitted maser rings. The bottom figures are color coded velocity images blue = 27.6 and red = 40.8 km/sec.; brightness is proportional to the square root of intensity. A velocity color bar is given at the bottom. The resolution ($490 \times 220 \mu\text{s}$, position angle -5°) is shown in the lower left corner of the top two sets of plots..

TABLE II
IK TAU SiO RING SIZES

Date	Phase	$\nu=1, J=1-0$ at 43.1 GHz					$\nu=2, J=1-0$ at 42.8 GHz				
		Maj (mas)	Min (mas)	PA (deg)	Width (mas)	Fract (%)	Maj (mas)	Min (mas)	PA (deg)	Width (mas)	Fract (%)
2004 Nov 08	0.53	35.7	32.1	6	4.2	69	35.0	31.4	6	4.1	78
2005 Oct 23	1.27	41.5	29.0	45	3.7	84	36.4	34.8	45	2.6	81
2006 Feb 03	1.49	44.3	35.4	32	2.4	87	41.4	34.4	32	2.0	82
2006 Apr 09	1.63	43.6	30.1	30	3.9	84	42.9	29.7	30	2.1	76
2006 May 28	1.73	44.5	35.6	38	3.6	77	43.1	35.6	38	3.5	72
2006 Sep 16	1.97	40.7	35.3	41	3.1	68	38.0	28.5	41	2.8	66
2010 Oct 17	5.14	39.3	34.0	-46	2.5	68	31.1	30.0	-46	2.1	67

- [2] W. D. Cotton, S. Ragland, W. C. Pluzhnik, E. and Danchi, W. Traub, L. A. Willson, and M. G. Lacasse, "SiO Masers in Asymmetric Miras III: IK Tauri," *ApJS*, vol. 187, pp. 107–118, 2010.

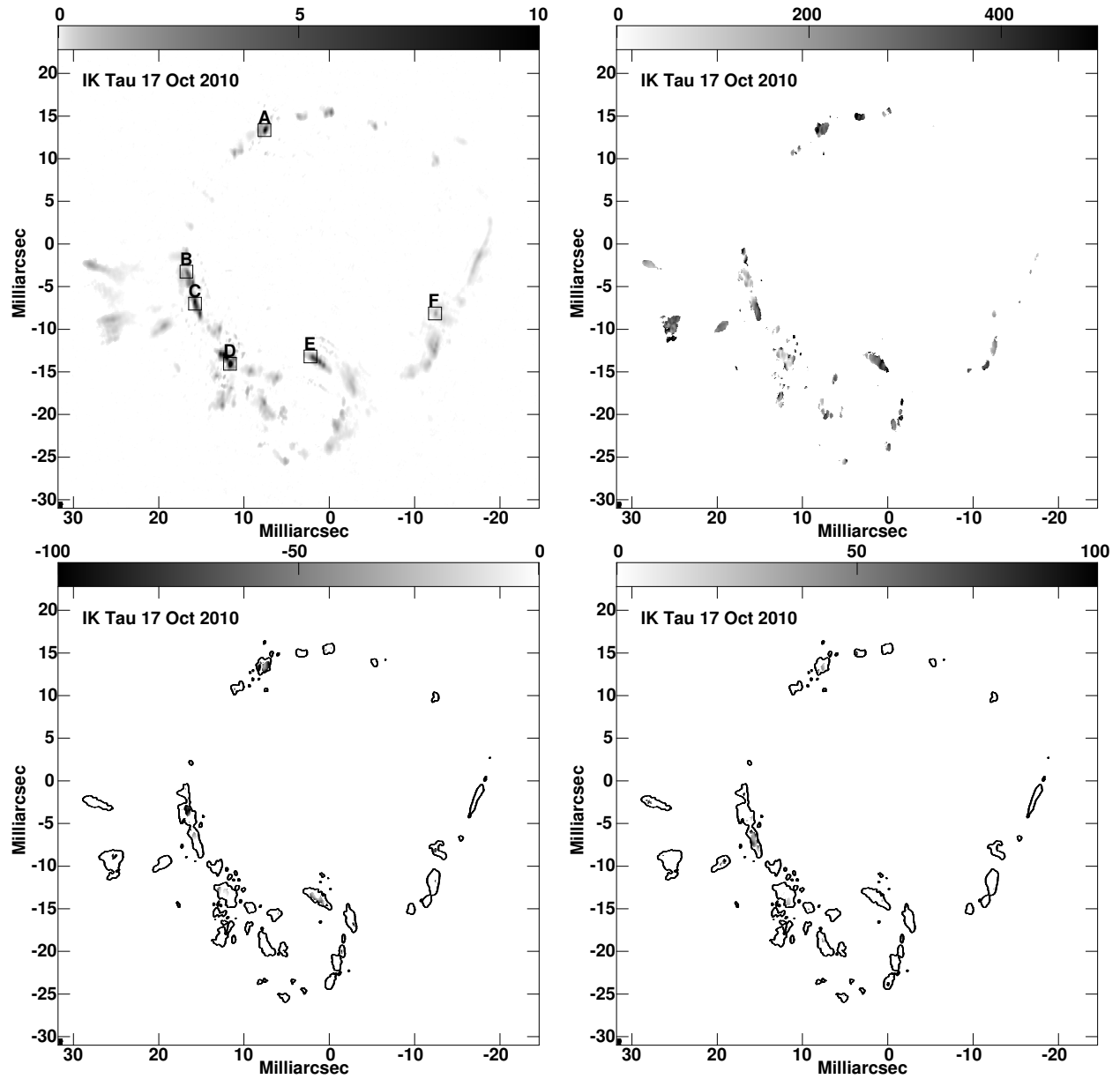


Fig. 4. Images of IK Tau, in the $\nu=2$, $J=1-0$ transition at 42.8 GHz. Top left is Stokes I showing locations where spectra are given. (center of square). Scale on top gives flux densities in Jy. Top right is the fractional linearly polarized emission; scale on top gives fractions in units of 0.001. Bottom left is the most negative fractional Stokes V in each pixel; scale on top gives fractions in units of 0.001; an outer Stokes I contour is overplotted. Bottom right is the most positive fractional Stokes V in each pixel; scale on top gives fractions in units of 0.001; an outer Stokes I contour is overplotted.

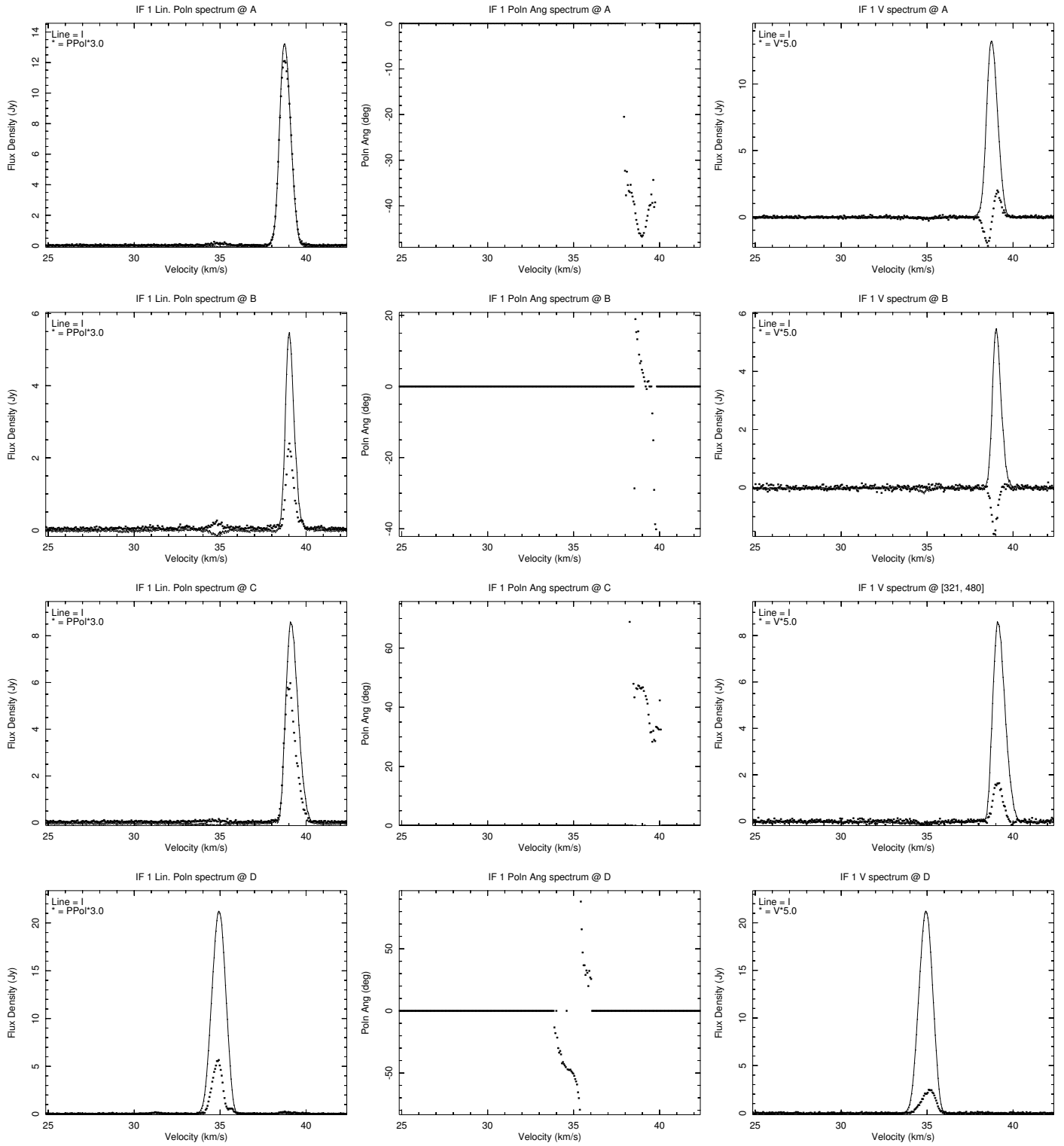


Fig. 5. Spot spectra in the $\nu=2, J=1-0$ transition at 42.8 GHz at locations shown in Figure 4. Stokes I is given as a line and Linear polarization ($\times 3$) in the left plots, Polarization angle in the center plots and Stokes V ($\times 5$) in the right plots are given as stars (*).

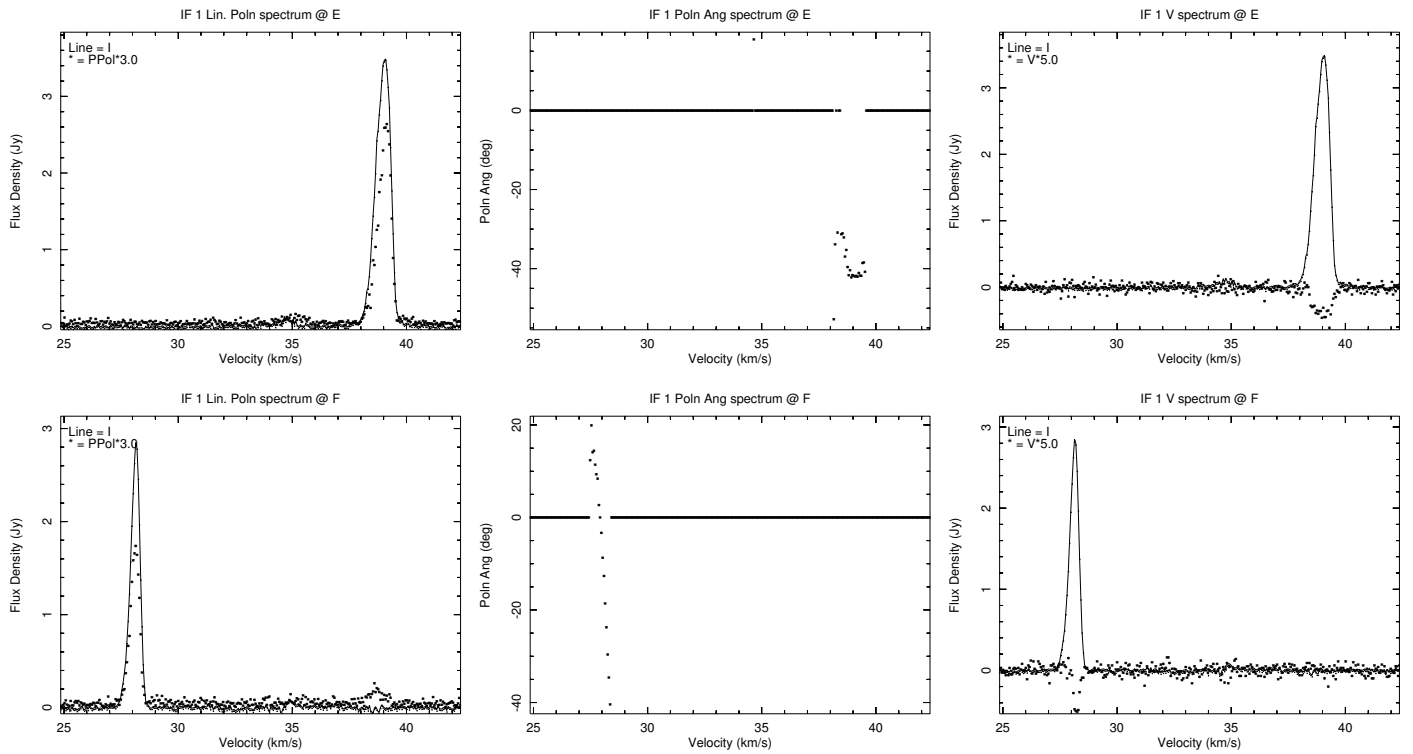


Fig. 6. More spot spectra in the $\nu=2, J=1-0$ transition at 42.8 GHz at locations shown in Figure 4. Stokes I is given as a line and Stokes V ($\times 5$) is given as stars (*).

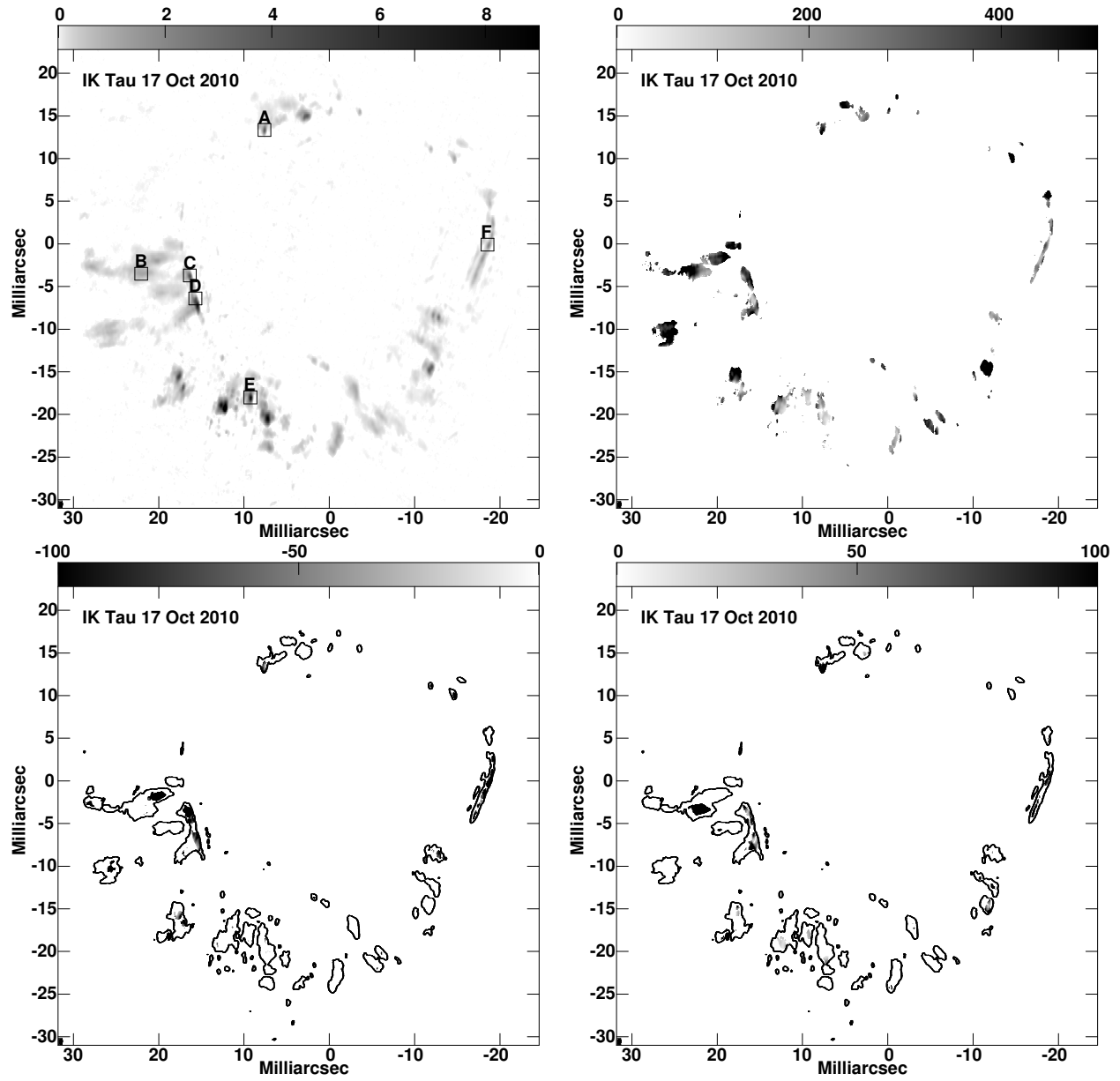


Fig. 7. Like Figure 4 but the $\nu=1, J=1-0$ transition at 43.1 GHz.

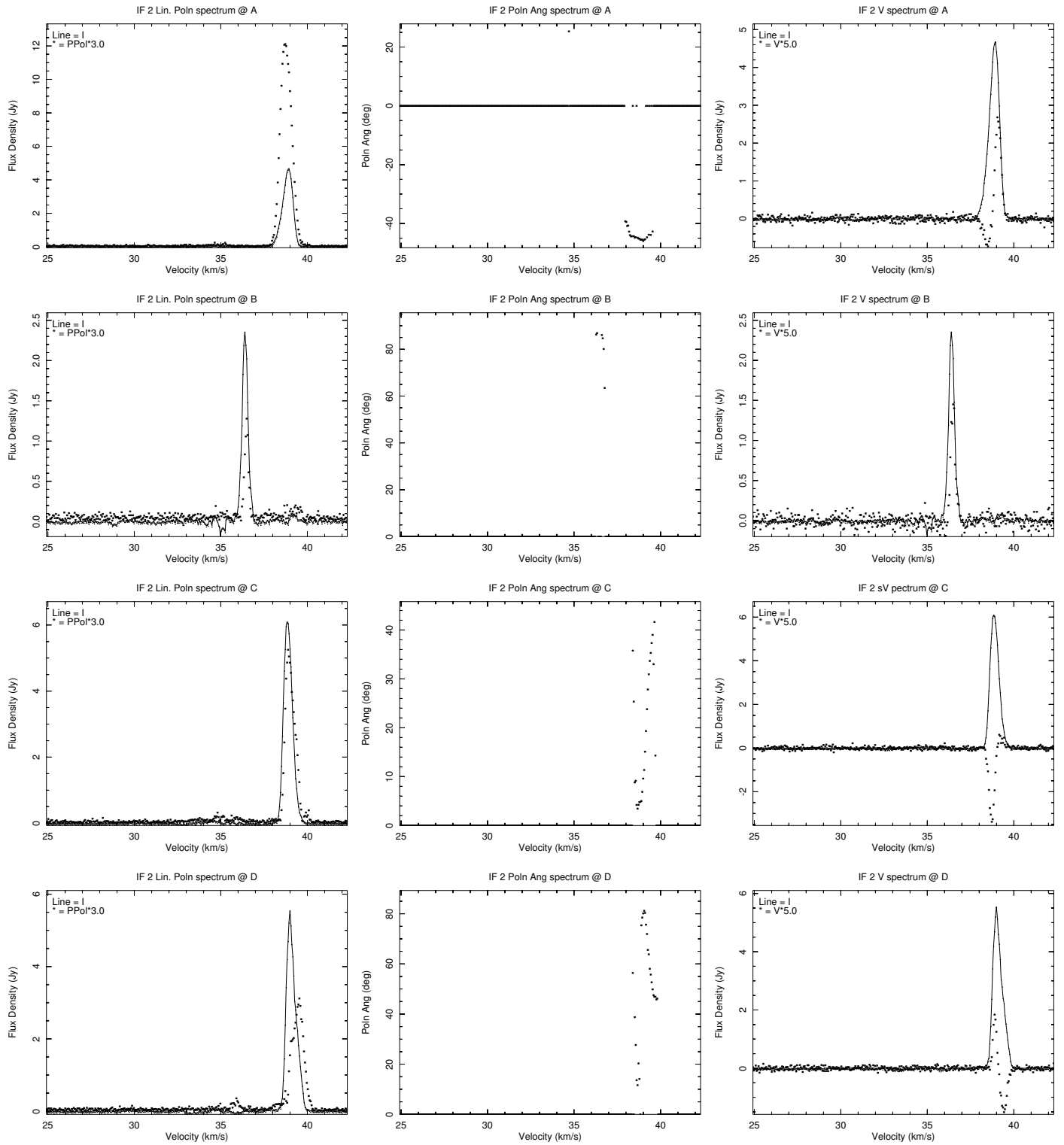


Fig. 8. Like Figure 5 but the $\nu=1, J=1-0$ transition at 43.1 GHz.

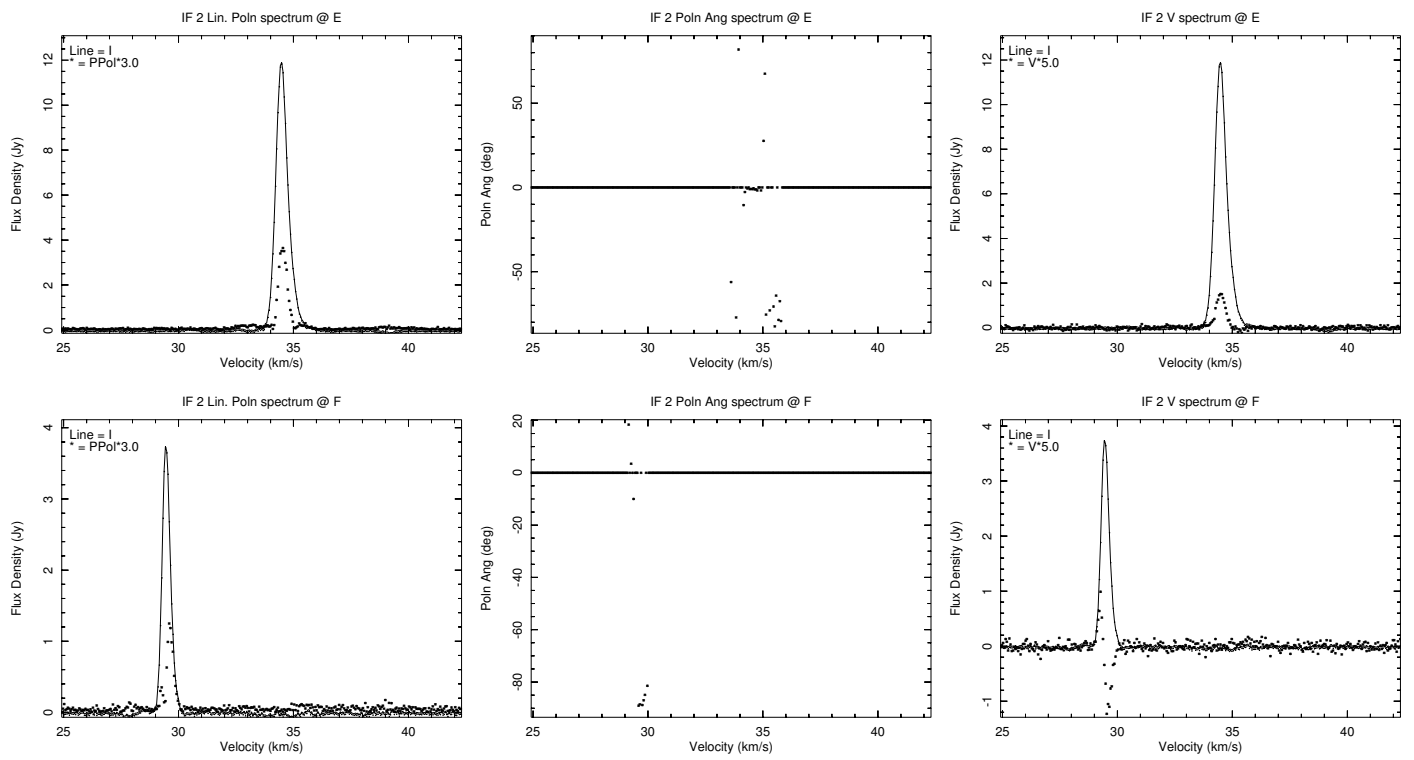


Fig. 9. Like Figure 8.